



Associated conference: 5th International Small Sample Test Techniques Conference

Conference location: Swansea University, Bay Campus

Conference date: 10th - 12 July 2018

How to cite: Holmström, S., Simonovski, I., Baraldi, D., & Bruchhausen, M., Altstadt, E., Delville, R., 2018. Successfully estimating tensile strength by small punch testing. *Ubiquity Proceedings*, 1(S1): 22 DOI: <https://doi.org/10.5334/uproc.22>

Published on: 10 September 2018

Copyright: © 2018 The Author(s). This is an open-access article distributed under the terms of the Creative Commons Attribution 4.0 International License (CC-BY 4.0), which permits unrestricted use, distribution, and reproduction in any medium, provided the original author and source are credited. See <http://creativecommons.org/licenses/by/4.0/>.

UBIQUITY PROCEEDINGS



<https://ubiquityproceedings.com>

Successfully estimating tensile strength by small punch testing

S. Holmström^{1*}, I. Simonovski¹, D. Baraldi¹, M. Bruchhausen¹, E. Altstadt², R. Delville³

¹ European Commission, Joint Research Centre, Petten, The Netherlands

² Helmholtz-Zentrum Dresden-Rossendorf (HZDR), Dresden, Germany

³ SCK-CEN Belgian Nuclear Research Centre, Mol, Belgium

* Correspondence: stefan.holmstrom@ec.europa.eu

Abstract: The Small Punch (SP) test is a relatively simple test well suited for material ranking and material property estimation in situations where standard testing is not possible or considered too material consuming. The material tensile properties, e.g. the ultimate tensile strength (UTS) and the proof strength are usually linearly correlated to the force-deflection behaviour of a SP test. However, if the test samples and test set-up dimensions are not according to standardized dimensions or the material ductility does not allow the SP sample to deform to the pre-defined displacements used in these correlations, the standard formulations can naturally not be used. Also, in cases where no supporting UTS data is available the applied correlation factors cannot be verified. In this paper a formulation is proposed that enables the estimation of UTS without supporting uniaxial tensile strength data for a range of materials, both for standard type and for curved (tube section) samples. The proposed equation was originally developed for estimating the equivalent stress in small punch creep but is also found to robustly estimate the UTS of several ductile ferritic, ferritic/martensitic and austenitic steels. It is also shown that the methodology can be further applied on non-standard test samples and test set-ups and to estimate the properties of less ductile materials such as 46% cold worked 15-15Ti cladding steel tubes. In the case of curved samples the UTS estimates have to be corrected for curvature to match the corresponding flat specimen behaviour. The geometrical correction factors are dependent on tube diameters and wall thicknesses and were determined by finite element simulations. The outcome of the testing and simulation work shows that the UTS can be robustly estimated both for flat samples as well as for thin walled tube samples. The usability of the SP testing and assessment method for estimating tensile strength of engineering steels in general and for nuclear claddings in specific has been verified.

Keywords: small punch testing, tensile strength, fuel claddings

1. Introduction

In a small punch (SP) test the local stresses and strains are biaxial in nature [1]. It has been shown to be a challenging task to estimate uniaxial (equivalent) stress from the force displacement curve of the SP test [2,3]. A new standard [4] is currently under preparation within the European Committee for Iron and Steel Standardization (ECISS), Technical Committee 101 (TC101), working group 1 (WG1) to replace the current CEN Workshop Agreement [5]. The new standard covers the classical Small Punch (SP) test for tensile property estimation and the Small Punch Creep (SPC) test for creep property evaluation. In this paper some new insight, gained from the SPC equivalent stress determination [6], is used for estimating the tensile strength.

In the SP test a hemispherical punch or a ball is forced at a constant displacement rate through a disc specimen (**Error! Reference source not found.**) that is clamped between an upper and a lower die. The main result of a SP test is the measured force F as a function of displacement v (at the punch tip) or deflection u (below the sample). The measured displacement v has to be corrected for compliance. The difference between displacement and deflection is the change of the specimen thickness at the punch tip.

Example SP force-displacement curves for the two standardized SP test set-ups and specimen sizes are shown in **Error! Reference source not found.**a and in normalized form in **Error! Reference source not found.**b.

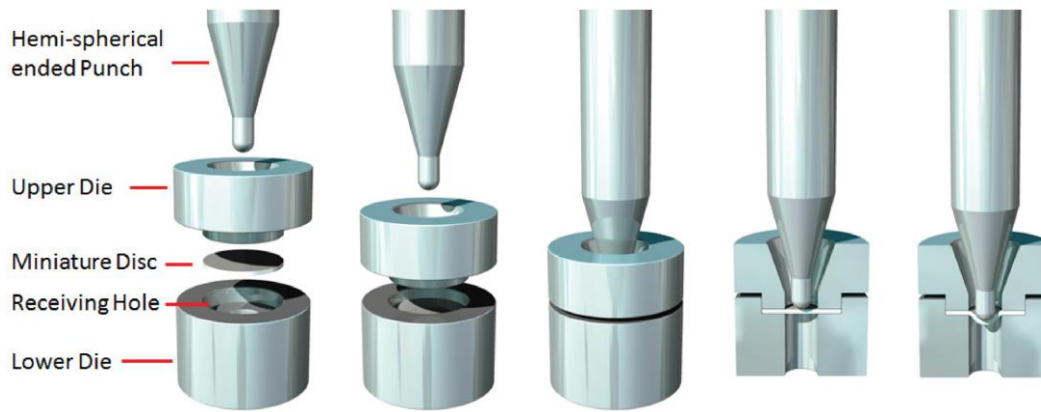


Figure 1. Schematic of a SP test set-up [7].

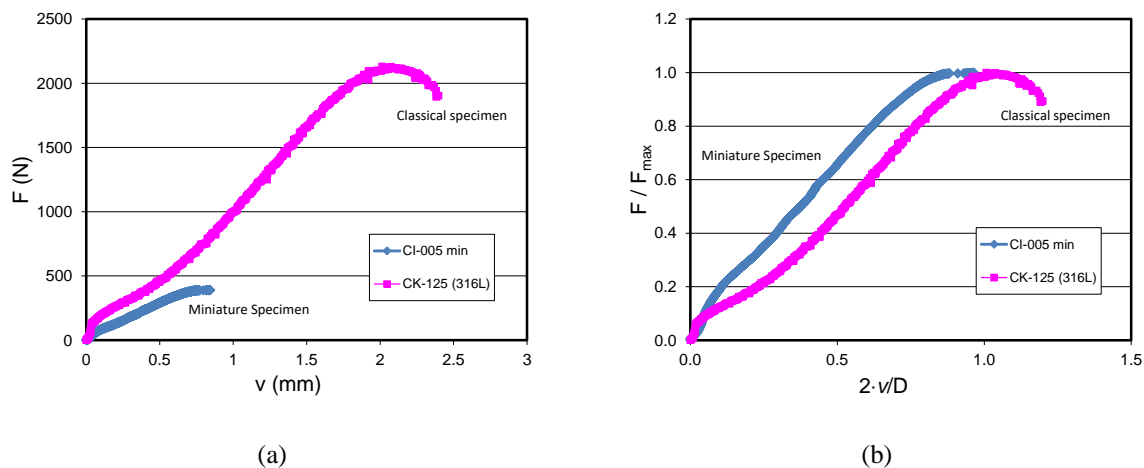


Figure 2. (a) Force-displacement curves for a standard 0.5 thick and a miniature 0.25 mm thick 316L steel sample [8] and (b) the corresponding normalized curves with force normalized with the maximum force F_{\max} and the displacement normalized by $2 \cdot v/D$, where D is the receiving hole diameter.

1.1 Test rig set-ups

The new standard (presented in [4]) includes two types of SP or SPC specimen, i.e. a specimen with a diameter $D_S = 8$ mm and an initial thickness $h_0 = 0.5$ mm and a specimen with $D_S=3$ mm and $h_0=0.25$ mm. The standard test rig specifics for these two types are given in **Error! Reference source not found.** together with other set-ups found in literature [2,5,11]. The lower die has a receiving hole with diameter D and a chamfer of length L . Both, D and L depend on the type of specimen used (**Error! Reference source not found.**).

Table 1. Main geometric characteristics of different SP test set-ups and specimen. Note that also a radius (instead of a chamfer (L)) can be used. The specimen and test set-ups given in bold are used in this paper.

Specification number SNR#	Test piece dimensions (D_s / h_0) [mm]	D [mm]	r [mm]	L [mm]	Note
#1	8/0.5	4	1.25	0.2	Standard set-up [2]
#2	8/0.5	4	1-1.25	0.2	CWA 15627 [2, 5]
#3	8/0.5	4	1-1.25 (1.19) ¹⁾	0.2	Japanese SPC [9]
#4	3/0.25	1.75	0.5	0.2	Standard set-up [2]
#5	3/0.25	2	0.5	0.2	MATTER [10]
#6	3/0.25	1.5	0.5	0.2	MATTER [10]
#7	Curved samples ²⁾	4	1.25	#N/A	Tube sections [11]

1) Kagoshima University uses $\varnothing 2.38$ mm balls

2) Curved tube samples: with outer diameters and wall thicknesses as in Table 1.

2. Materials

The materials assessed here are from various projects and test campaigns as given under the sub-headings below. The test materials and their room temperature (RT) ultimate tensile strengths are given in Tables 2-4. These values are estimated by SP tests later in this paper.

2.1 ECISS/TC101 round robin materials

The main materials used by ECISS/TC101/WG1 for the estimation of tensile properties were different heat treatments of P92 pipe. To study the impact of differing yield to tensile strength ratios the 316L was also tested. The TC101 test materials are given in Table 2. All the ECISS/TC101/WG1 materials, except 316L-miniature, are tested at room temperature with test specification number $S_{NR\#1}$ (**Error! Reference source not found.**) and the miniature test sample with $S_{NR\#4}$.

Table 2. TC101 materials and their ultimate tensile strength at room temperature.

Material and designation	Uniaxial Rm (MPa) at RT
P92– as received	808 ¹⁾ ,
P92– Heat treatment 1	675 ¹⁾
P92– Heat treatment 2	707 ¹⁾
P92– Heat treatment 3	726 ¹⁾
P92– Heat treatment 4	733 ¹⁾
316L – miniature	569 ²⁾
316L	569 ²⁾

1) As given by material supplier (MMV).

2) As measured by JRC [8].

2.2 TASTE project materials

In the EERA JPNM pilot project TASTE [11-13] the main material of interest was the nuclear grade titanium stabilized 15-15Ti (DIN 1.4970) stainless steel cladding [14]. The 15-15Ti is the primary choice for fuel cladding of several current fast spectrum research reactor projects. The main test material was the 24% cold worked (24%CW) 15-15Ti cladding tube material, manufactured by Sandvik on behalf of SCK•CEN. The material batch has passed tight quality control, i.e. stringent composition, grain sizes and mechanical properties (yield strength, tensile strength and elongation at rupture) control and tight product tolerances (diameters, straightness and ovality), roughness and defect controls. A smaller batch with a cold-work level of 46% (46%CW) was also produced and tested. For the 46%CW the deformation level is intended to simulate irradiation damaged material in the sense of work-hardening saturation demonstrated by the small difference between the proof stress and the ultimate tensile strength. The 46%CW also has markedly decreased total elongation [15,16].

The 15-15Ti material properties (axial) at RT performed on full tubes (no waist) and on sections cut from the wall (with waist) are given in 3 together with the properties of the reference material P91. All the JRC curved specimens analyzed for this paper were tested with a test-set-up with $D=4$ mm, $r=1.25$ mm and no chamfer ($S_{NR\#7}$ in **Error! Reference source not found.**). The chamfer cannot be manufactured on a curved surface. The flat reference P91 specimens were tested with the standard test set-up ($S_{NR\#1}$ in **Error! Reference source not found.**), with the standard thickness ($h_0=0.5$ mm), and with a reduced thickness to comply with the tube specimen, i.e. $h_0=0.45$ mm. The flat test set-up always has a chamfer (Table 3).

Table 3. TASTE project materials, sample types (inner diameter ID or flat) and their ultimate tensile strengths at RT.

Material and designation	Tube ID / h ₀ D / h ₀ (mm)	Uniaxial R _m (MPa) at RT
15-15Ti CW24% CURVED	6.55 / 0.45	810 ¹⁾ 857 ²⁾
15-15Ti CW46% CURVED	6.55 / 0.45	925 ¹⁾ 929 ²⁾
P91 CURVED	6.55 / 0.45 ⁴⁾	680 ³⁾
P91 FLAT	Flat/0.45 Flat/0.50	680 ³⁾

1) As given by the material supplier [11], tested on full tube.

2) As measured from axial tube samples [15, 16], tested on tube section.

3) As measured from standard size uniaxial samples [17].

4) Inner surface as from EDM cut.

2.3 ASTM round robin materials

In the US the American Society for Testing and Materials (ASTM) has an ongoing work item [18] for the development of a SP standard. The scope of the work is to enable estimates of yield and tensile strength up to a temperature of 450°C for metallic materials. JRC has taken part in this effort as a member of an inter-laboratory round-robin testing. The tested steels are given in Table 4. The measured UTS and proof stresses were not provided until after the delivery of the test data and the tensile property estimates.

Table 4. All materials tested at RT with specimen Ø8 mm; h₀=0.500 mm and a test-set-up with D=4 mm, r=1.25 mm and L=0.2 mm (S_{NR}#1).

Material and designation	Uniaxial R _m (MPa) at RT
A533B	625
A533B (batch 2)	635
COST F	852
22K	498
10Kh11N20T3R	958
08Kh18N10T	560
15Kh2MFA	986

3. Classical and recently developed estimation procedures for force to stress conversion

The simplest force to stress conversion can be found in the CEN Work Shop Agreement (CWA, Code of Practice) [5]. The conversion is meant for small punch creep (SPC) test giving a constant force to stress ratio $\Psi = F/\sigma$, allowing for different test set-up dimensions and specimen thicknesses. The CWA equivalent creep stress σ_{SPC} can be calculated as:

$$\sigma_{SPC} = \frac{F_{SPC}}{3.33 \cdot k_{SP} \cdot R^{-0.2} \cdot r^{1.2} \cdot h_0} \text{ MPa} \quad (1)$$

where F_{SPC} (in N) is the SPC test force (load), h_0 the initial specimen thickness, k_{SP} a “ductility” parameter and r , R are the puncher radius and receiving hole radius (in mm) as given in **Error! Reference source not found.**. For the standard test set-up (S_{NR}#1) the $\Psi_{CWA}=1.895$ when $k_{SP}=1$. This conversion factor works well for steels like P91, where the minimum deflection rate is reached at a deflection of around 1 mm. The draw-back of this method is that k_{SP} is not a constant and it can be both temperature and force dependent [18].

The CWA model is based on the Chakrabarty [1] membrane stretch equations. The Chakrabarty (CHA) model gives the Ψ_{CHA} as a function of displacement v . Full CHA curves can be defined for each test set-up using the equations given in [1]. The maximum $\Psi_{CHA-max}$ at $v_{CHA-max}$ can be calculated with Eq. (1). The $\Psi_{CHA}=\Psi_{CWA}$ at a displacement $v_{max}=1.58$ mm for the standard test set-up and specimen size (S_{NR}#1).

The corresponding classical equation (CLA) in [5] for estimating the (uniaxial) ultimate tensile strength R_m with small punch “tensile” tests (SP) is:

$$R_{m-CLA} = \beta_{Rm-CLA} \cdot \frac{F_m}{h_0 \cdot u_m} \text{ MPa} \quad (2)$$

where F_m (in N) is the maximum force reached during the test and β_{Rm-CLA} is a geometry dependent correlation coefficient which needs to be determined. The main draw-back of this method is that the β_{Rm-CLA} has to be established by correlation to actual uniaxial tensile tests or by Finite Element Analysis (FEA) simulation with the right constitutive equations in place. It has been found that the correlation factor seems to be somewhat material dependent but mainly test-setup and specimen thickness dependent. In this paper the classical model (CLA) is used for estimating tensile strength as in Eq. (2), with a constant value for $\beta_{Rm-CLA} = 0.276$, optimized in the MATTER project [19] for P91 steel for the standard test set-up and a specimen thickness of 0.5 mm.

The above method seemingly works well for ductile materials but does not give adequate results for less ductile materials failing at deflections well below $v_{CHA-max}$. For less ductile materials other methods have to be applied.

A new promising method for both ductile and less ductile materials has been proposed by Altstadt et al. [3] and it has been included in the new standard as an Annex. The Altstadt method (ALT), optimized on finite element simulated materials, correlates the force F_i to the ultimate tensile strength at a much lower displacement v_i in the force-displacement curve. The ALT model correlation to the tensile strength is:

$$R_{m-ALT} = \beta_{Rm-ALT} \cdot \frac{F_i}{h_0^2} \text{ MPa} \quad (3)$$

The F_i (in N) of the ALT method is extracted from the test data at the displacement $v_i=0.645$ mm or a deflection of $u_i=0.55$ mm. The model parameters are to date only defined for the $S_{NR\#1}$ and $S_{NR\#4}$ test set-ups (see **Error! Reference source not found.**). The correlation coefficient β_{Rm-ALT} is 0.179 for $S_{NR\#1}$. This is an average value for a range of simulated materials with different tensile strengths and ductilities.

In [6] the Empirical Force to Stress (EFS) model and the Modified Chakrabarty (MCH) model was shown to robustly estimate the equivalent creep stresses for equal creep rupture times of SPC and uniaxial creep tests. The MCH is a simplification of the EFS model that can be recalculated for different test set-ups since the model parameters can be determined analytically using the CHA as base.

The Ψ_{MCH} is:

$$\Psi_{MCH} = A + B \cdot v \text{ [N/MPa]} \quad (4)$$

where v is the displacement (or deflection) and A and B are test set-up dependent constants. In the case of small punch creep v is replaced by u_{min} , i.e. the deflection where a minimum deflection rate is reached in a test. The SPC data determined constants (from [6]) for A and B which are applied unchanged on the SP test data with the standard test-setup and specimen thickness, i.e. $A=0.6143$ and $B=1.2954$ for the $S_{NR\#1}$ set-up. For the curved specimen, the miniature sample and the 0.45 mm thick standard SP specimen the constants have been recalculated using the methodology given in [6]. For the curved specimen further correction factors have to be applied as described in section 3.2 in this paper.

In Figure3a it is shown that the calculated F_i and v_i (and corresponding u_i) from [3] that was the base for Eq. (3) are in good agreement with the Ψ_{MCH} curve for the standard specimen and standard test-set up. In Figure3b it can be seen that for the miniature specimen the MCH slope is representative of the F_i/v_i (and F_i/u_i) but the analytically calculated MCH intercept is somewhat high. It is to be noted that Ψ_{MCH} curve for this specimen size and test-setup ($S_{NR\#4}$) has not been verified up to now by creep tests and the few SP tests indicate that the model overpredicts the UTS (see section 4). The discrepancy is likely to be caused by the assumed fixed point for the MCH set by the CHA model v_{max} , i.e. $\Psi_{MCH}(v_{max}) = \Psi_{CHA}(v_{max}) \cdot (1+h/r)$. This factor was optimized on P91 steel [18]. If another more reliable fixed point can be found, such as using the ALT data or actual test data (both SP and SPC data) it is foreseen that the MCH model for the miniature specimen can be improved. It is to be emphasized that the MCH model is not restricted to the location of maximum force as the CLA model even if it has been used that way in this paper. It can be used as the ALT model at lower displacements. This feature will be studied in future work.

All the above stress conversion models for the SNR#1 test-setup are shown in Figure4 with P91 SP data from the MATTER project.

Unification of reference stress estimation between SPC and SP tests would have a beneficial effect on the credibility of the SP and SPC determined material properties.

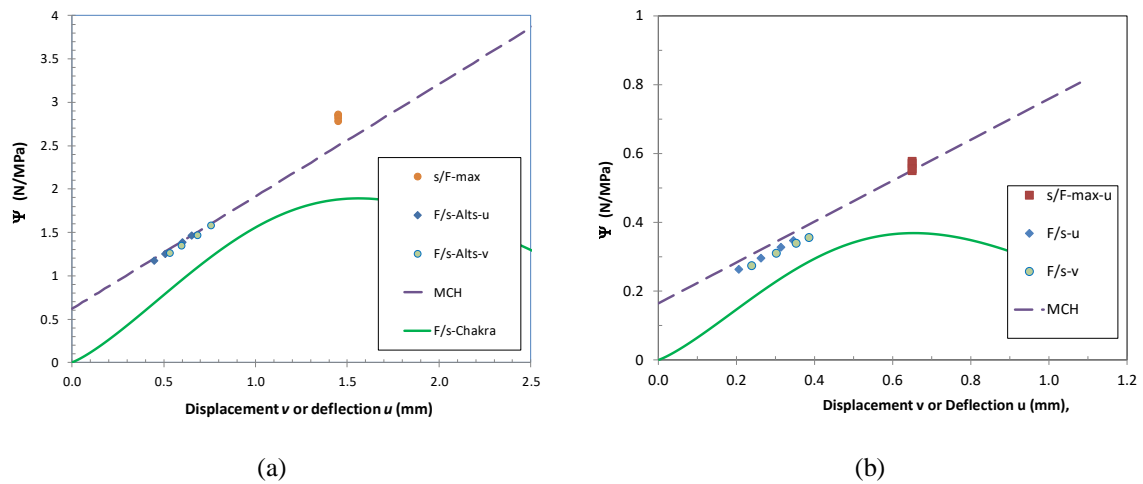


Figure 3. Force over stress (Ψ) as a function of v or u according to the classical Chakrabarty (CHA) and the MCH model for SP and SPC reference creep stress determination. The F_i / R_m and F_{max} / R_m of the simulated materials from the ALT model [3] are also shown for a) set-up $S_{NR}\#1$ and b) $S_{NR}\#4$.

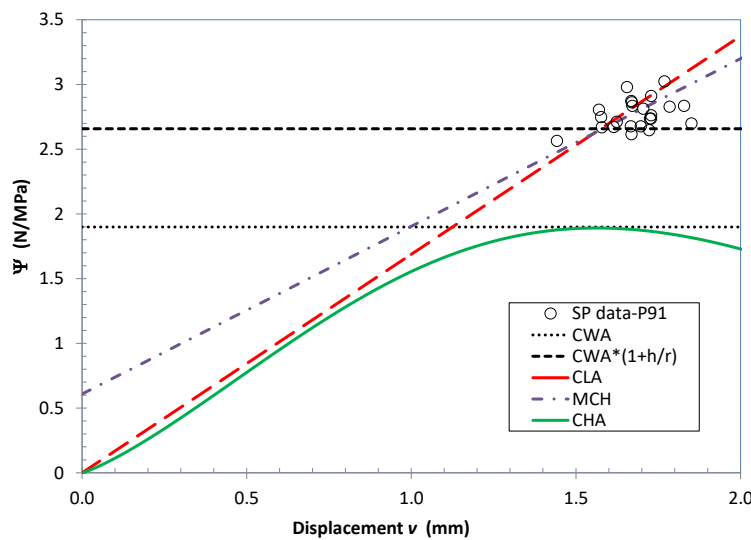


Figure 4. Force over stress (Ψ) for the SPC and SP models, Eqs. (1,2, 4) as a function of v . The shown F_{max}/R_m data are from the MATTER project.

3.1 Correction for curvature for thin walled tube samples

When SP testing curved samples [11,21] it is evident that the force-displacement curves are different from those of flat specimens. To find the right way of correcting the deflections (and marginally the force) a number of 3D FEA simulations using ABAQUS [22] have been performed on $1/4$ of the geometry for simulated flat and curved specimens. The curved sample studied in this paper is a section of the aforementioned SCK-CEN tube. The geometrical configuration consisting of the top die (red), specimen (blue), bottom die (grey) and the spherical punch (green) is shown in Figure 5. Example of computed force-displacement curves for the studied materials is shown in Figure 6. A more detailed description of the methodology and resulting correction factors are given in [23].

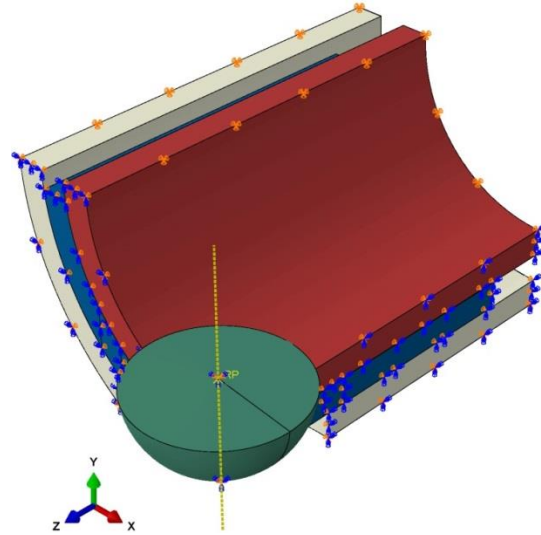


Figure 5. Quarter symmetry FEA model of the SP test on curved (cladding tube) specimen [23].

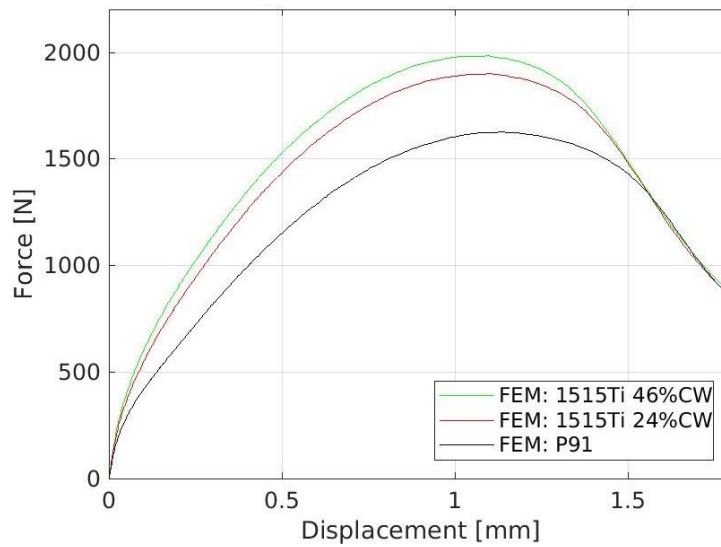


Figure 6. FEA computed force-displacement responses for P91, 24% CW and 46% CW 15-15Ti curved samples from cladding tubes. The friction coefficient, $\mu=0.2$ and the specimen thickness 0.45 mm.

To obtain the equivalent force and displacement of a flat specimen, the measured force and displacement of a SCK-CEN tube specimen should be divided by a factor of 1.07 and 0.71, respectively. The given factors are averages on the results acquired from the two 15-15Ti materials and the reference material P91.

4. Results

The ultimate tensile strengths estimated by SP tests are given in Tables 5-7 as relative errors of the uniaxial UTS values given in Tables 2-4.

The relative error E_{rel} is calculated as:

$$E_{rel} = \frac{R_{m-SP}}{R_{m-UA}} - 1 \quad (4)$$

Where R_{m-UA} is the uniaxial tensile strength, R_{m-SP} the estimated UTS calculated by the CLA, ALT and MCH models.

Note that for the curved samples there are currently no calculated v_i values at which one could extract the F_i values for the ALT model. Potentially the same correction factors could be used as for correcting the v_{max} and F_{max} but this has not been attempted in this work.

Table 5. The UTS estimate relative errors, Eq. (4), for the ASTM round robin materials at RT.

Material and designation	CLA ¹⁾	ALT (v)	MCH (v)
A533B	-9%	-1%	-9%
A533B (batch 2)	-10%	-1%	-9%
COST F	-7%	2%	-7%
22K	-4%	-7%	-2%
10Kh11N20T3R	-5%	-3%	-5%
08Kh18N10T	6%	-24%	13%
15Kh2MFA	-17%	-9%	-17%

1) Correlation constant for CLA model ($\beta_{R_m-CLA}=0.297$, Eq. (2)) from MATTER, optimized on P91 by JRC.

Note that the R_m estimates from CLA and the MCH are more or less the same. This is to be expected if the displacement at maximum is around 1.6 mm. The ALT estimates are for some materials more accurate but the model seems to be prone to larger deviations, especially for ductile material.

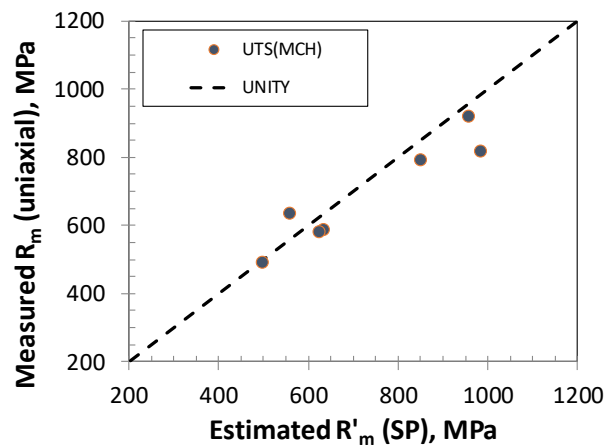


Figure 7. Estimated vs measured uniaxial axial strength at RT for all ASTM materials in Table at RT using the MCH model.

Table 6. Calculated relative errors, Eq. (4), for JRC tests at RT for the ECISS/TC101/WG1 materials.

Material and designation	CLA ¹⁾	ALT (v)	MCH (v)
P92– as received	7%	3%	3%
P92– Heat treatment 1	9%	-2%	6%
P92– Heat treatment 2	13%	-7%	8%
P92– Heat treatment 3	12%	-5%	6%
P92– Heat treatment 4	6%	0.3%	2%
316L – miniature	-3% ²⁾	23%	14% ³⁾
316L	10%	-26%	18%

1) Correlation constant for CLA model ($\beta_{R_m-CLA}=0.297$, Eq. (2)) from MATTER, optimized on P91 by JRC

2) Correlation constant from miniature specimen CLA model by HZDR ($\beta_{R_m-CLA}=0.26$, Eq. (2))

3) MCH model parameters as in Figure 7.

The ALT and MCH models are for these sets of data better than the CLA model, except for the miniature specimen estimate. It is to be noted that the MCH is generally over-predicting the stress though less so than the CLA model.

Table 7. Calculated relative errors, Eq. (4), for JRC tests at RT for the TASTE materials.

Material and designation	CLA	MCH
15-15Ti CW24% CURVED	3%	-2%
15-15Ti CW46% CURVED	10%	-1%
P91-CURVED (0.45 mm thick)	-8%	-6%
P91 standard specimen (0.45 mm thick)	-5%	-2%
P91 standard specimen (0.5 mm thick)	-2%	-2%

In addition to the RT tests the MCH method was also applied to the full range of test temperatures, i.e. RT-800°C. The results are very encouraging as can be seen in Figure 8. In the previous assessments on the TASTE data [11] the SP estimates were based on a displacement corrected CLA model, with inherently more scatter in the estimated UTS. The CLA model also predicts somewhat lower strengths for P91 and clearly over-predicts the RT strength for the 46%CW 15-15Ti steel.

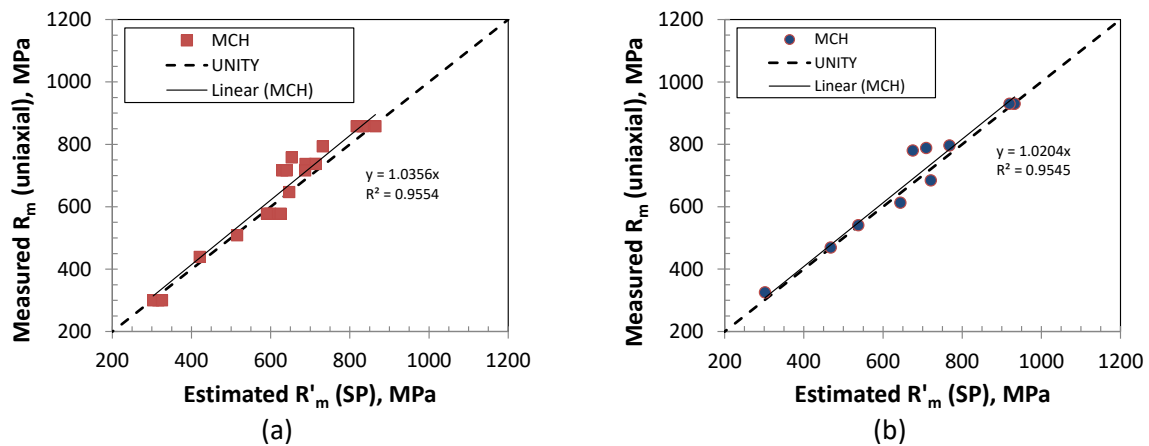


Figure 8. Estimated vs measured uniaxial axial strength for a) 24%CW and b) 46%CW 15-15Ti using the MCH model in the temperature range RT-800°C.

In Figure 9 the reference P91 SP estimates are plotted against the measured uniaxial strength for the temperature range RT-650°C. It can be seen that the P91 flat specimens give robust predictions and the spark erosion manufactured curved samples show more scatter. The MCH seems to under-predict the tensile strength for the curved P91 samples. This could be an artefact caused by the manufacturing route, i.e. the inner surface was not polished.

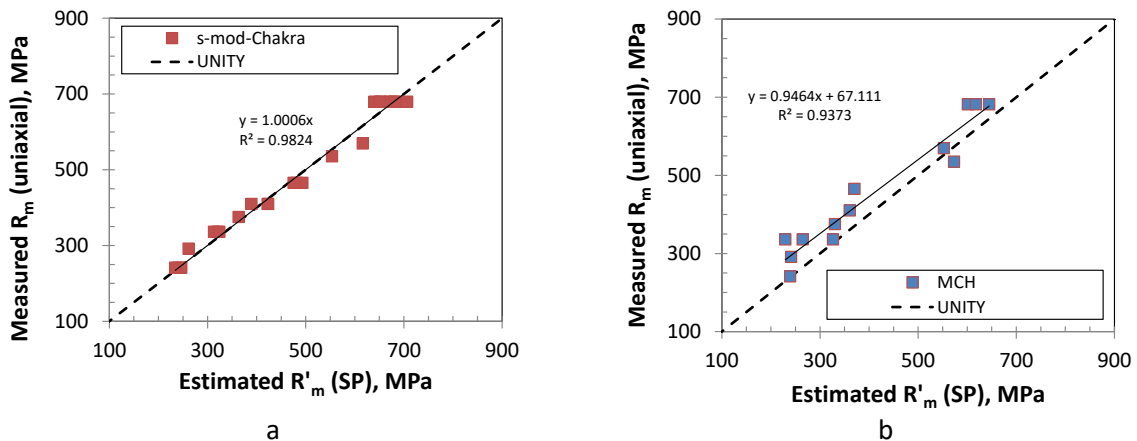


Figure 9. Estimated vs measured uniaxial axial strength for P91 steel a) standard flat specimen and b) EDM cut curved samples in the temperature range RT-650°C.

In Figure 10 and Figure 11 the SP estimated strengths are plotted as a function of temperature together with both uniaxial UTS results and hoop direction ring tension results for 24%CW and 46%CW samples correspondingly.

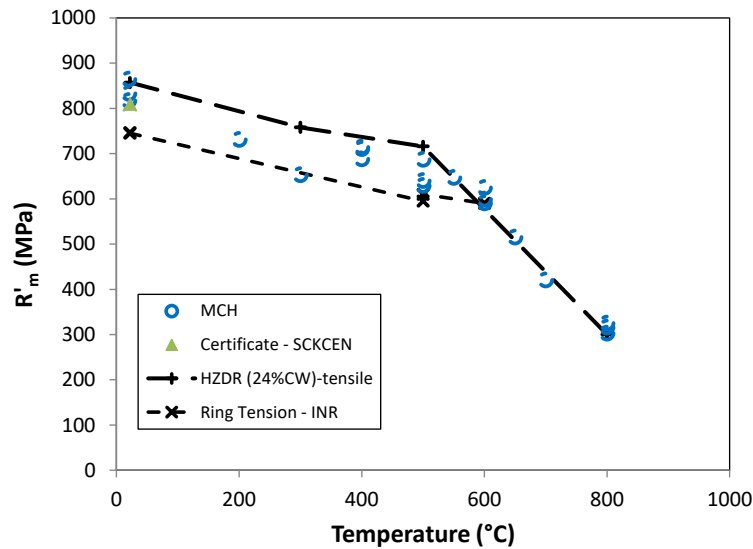


Figure 10. Comparison of RT-800°C tensile strength estimates for 24% CW 15-15Ti from sub-sized axial specimen, Ring-Tension and the new estimates based on the SP data [24] assessed with the MCH model.

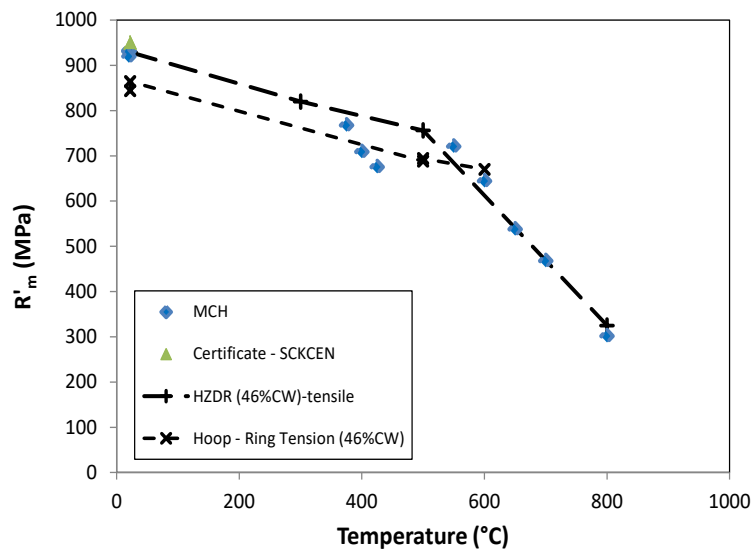


Figure 11. Comparison of RT-800°C tensile strength estimates for 46% CW 15-15Ti from sub-sized axial specimen, Ring-Tension and the new estimates based on the SP data [25] assessed with the MCH model.

5. Discussion

The models compared in this paper for SP estimation of the UTS include a model originally optimized for SPC creep data assessment. It is encouraging to find that the same formulation gives good estimates also when applied on SP data for estimating the tensile strength. In Figure 12 the SPC data from the ECISS/TC101/WG1 round robin [6] show the $\Psi = F_{SPC} / \sigma_{c-UA}$ ratio as a function of the measured deflection at minimum deflection rate (u_{min}) for 3 different materials, i.e. a P92 pipe, a F92 forging and a 316L plate. The MCH line is calculated on the standard test-setup and a 0.5 mm specimen thickness. In Figure 13 the SP data from the TASTE project (assessed in this paper) is presented as $\Psi = F_m / R_{m-UA}$ as a function of displacement v_m (v at F_m). In this case the MCH was modified to fit the standard test-setup with a 0.45 mm specimen.

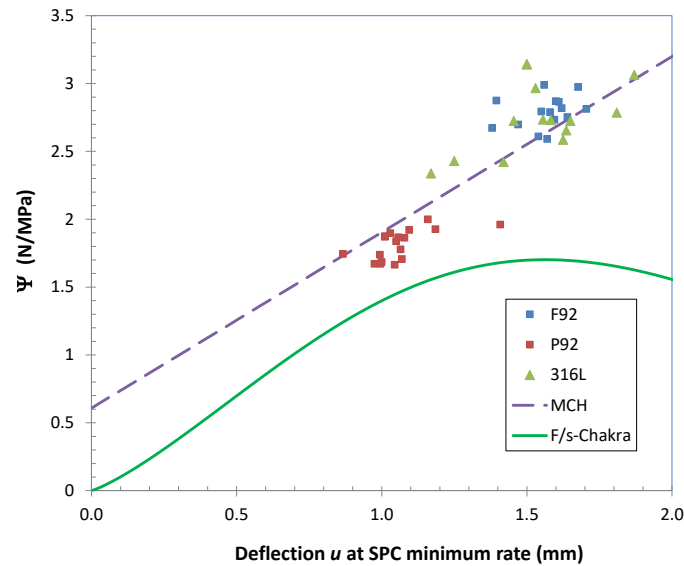


Figure 12. The SPC creep data from the ECISS/TC101/WG1 round robin [6] plotted as Ψ at u_{min} together with the CHA and the MCH models. Note that the P92 SPC samples were suffering from early cracking and failure. The predicted uniaxial creep stress at equal rupture time will therefore be increased and Ψ decreased. The specimen thickness $h_0=0.5$ mm.

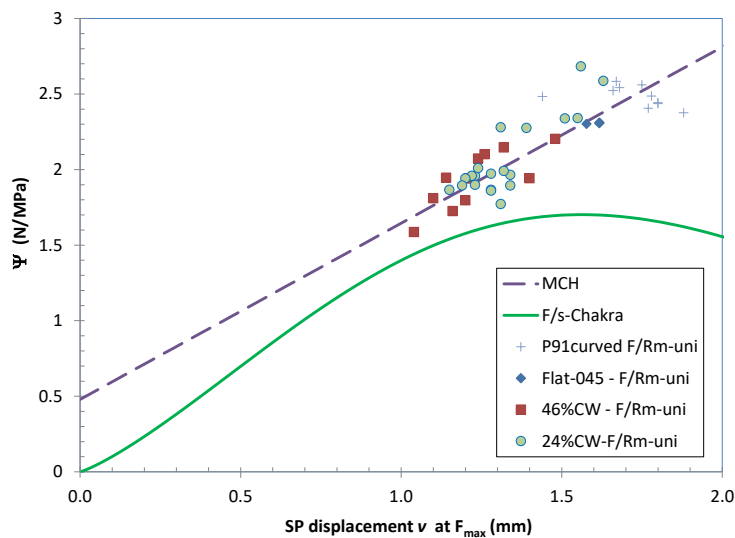


Figure 13. The SP test data from the TASTE project plotted as F_{max}/R_{m-UA} at the test specific v_{max} . Note that $h_0=0.45$ mm.

It could be concluded from the above figures that the MCH could be given a slightly steeper slope, perhaps pivoting around a displacement of 1 to 1.25 mm. However, the slope should not be as steep as CLA model, having a slope of h_0/β_{Rm-CLA} going through the origin. The CLA model is not giving an optimal solution if applied on SPC data replacing v_{max} for u_{min} .

As stated earlier, the optimization of the MCH model parameters using both SPC and SP data would most likely improve the understanding and accuracy of predictions for both small punch test types.

Studying the F_i/R_m for the ALT model, as seen in Figure 14, for the ASTM steels it is evident that some of the materials with low proof strength did not give the expected Ψ as was indicated by the FEA simulated SP tests on “synthetic” materials. It could be concluded that for low proof stress materials the R_m cannot be estimated at this (low) displacement. Maybe this information can instead be used for improving the SP estimates for proof strength.

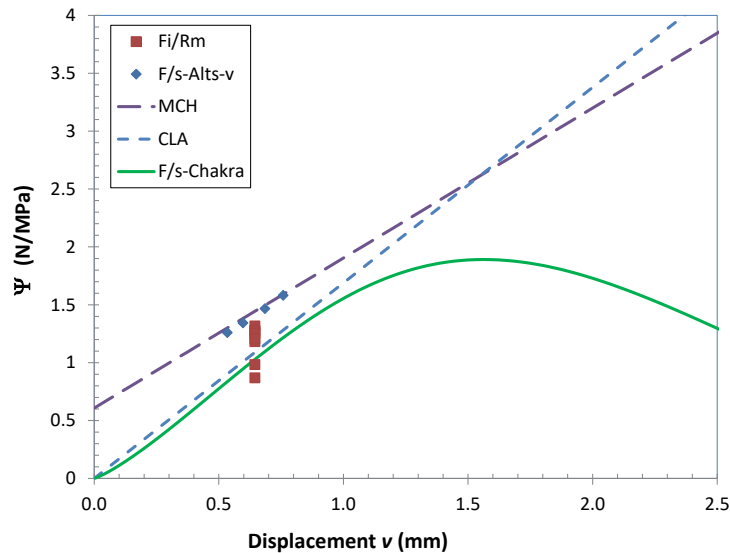


Figure 14. Room temperature F_i/R_m data from the ASTM materials extracted from the force displacement curve at $v_i=0.645$.

One of the remaining main challenges for increasing the applicability of the SP tests technique in general is to establish ductility limitations for successful assessment of both SP and SPC data. For instance what is the impact of material “necking” on the SP test curve. For some low ductility materials this could happen already at small displacement [26]. The material properties beyond the uniaxial engineering ultimate tensile strength, i.e. after necking, will naturally have an effect on v_{max} and F_{max} . In Figure 15a a SP tested 15-15Ti specimen clearly failed by plastic collapse whereas the SPC specimen in Figure 15b has cracked open in a star shaped manner. The change in fracture behavior is linked to the deformation rate and differences in tensile and creep ductility.

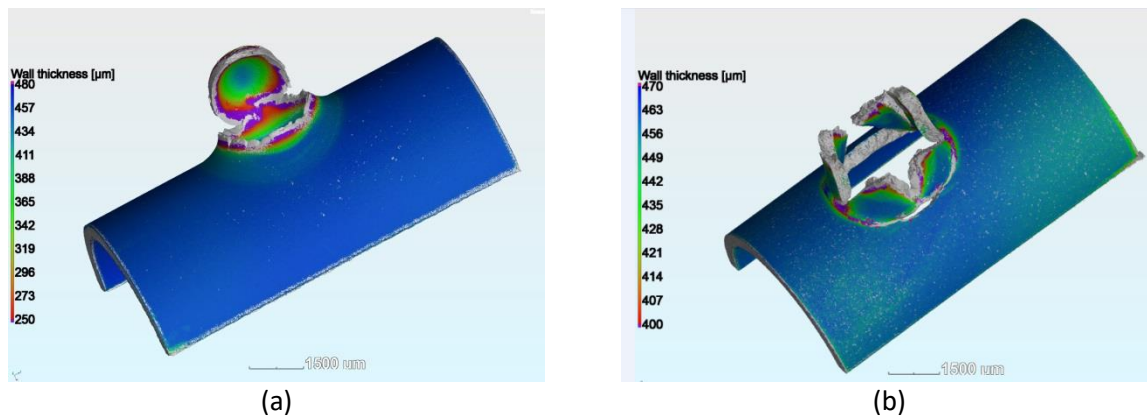


Figure 15. Difference in fracture mode of a 24%CW 1515Ti A) SP “tensile” specimen after test at 600°C and B) SPC creep specimen ruptured after 22 h at 600°C/400N.

6. Conclusions

A range of different materials with differing tensile strengths have been analyzed with three different models. SP data from test set-ups that are non-standard in nature such as the curved samples from fuel cladding tubes have also been successfully assessed. The conclusions to be drawn from results from the here presented assessments are:

- Good estimates on the tensile strength can be acquired by the existing conversion models, e.g. the ALT model developed for SP data and the MCH model initially developed for SPC data.
- The force to stress conversion of SP and SPC test can be unified by optimizing models like the MCH.
- Curved samples such as cladding tubes can be tested by SP and analyzed successfully using curvature corrections calculated by FEA.

- Tensile strength estimates for less ductile materials should be done on forces extracted at low displacement, for instance using an ALT type model.
- Challenges remain in the field of improving the estimates on proof strength and ductility.

It could be claimed that the usability of the SP testing has been improved greatly by the new assessment methods, such as for estimating tensile strength in general and for nuclear claddings in specifically.

References

1. Chakrabarty, J., A theory of stretch forming over hemispherical punch heads, *International Journal of Mechanical Sciences* 12(4), pp.315-325, 1970.
2. García, T.E.; Rodríguez, C.; Belzunce, F.J.; Suárez, C., Estimation of the mechanical properties of metallic materials by means of the small punch test. *Journal of Alloys and Compounds* 582:708–717, 2014.
3. Altstadt E.; Houska M.; Simonovski, I.; Bruchhausen, M.; Holmström, S.; Lacalle, R., On the estimation of ultimate tensile stress from small punch testing, *International Journal of Mechanical Sciences* 136, pp. 85–93, 2018.
4. Bruchhausen, M.; Austin, T.; Holmström, S.; Altstadt, E.; Dymacek, P.; Jeffs, S.; Lancaster, R.; Lacalle, R.; Matocha, K.; Petzova, J., European standard on small punch testing of metallic materials. In Proceedings of the ASME 2017 Pressure Vessels & Piping Conference, Volume 1A-2017, Waikoloa Village, USA, July 16-20 2017.
5. CEN Workshop Agreement CWA 15627: Small Punch Test Method for Metallic Materials: European Committee for Standardization, CWA 15627: 2007.
6. Holmstrom et. Al, Creep strength and minimum strain rate estimation from Small Punch Creep tests, MSEA-2018-01831, to be published.
7. Lancaster, R.; Davies, G.; Illsley, H.; Jeffs, S.; Baxter, G. 2016. "Structural integrity of an electron beam melted titanium alloy". *Materials*, 9(6), p. 470.
8. [Catalog] Holmstrom, S.; La-Petite, J.-M.; De Haan, F.; SP tests at room temperature on 316L, version 1.0, European Commission JRC, 2018, <http://dx.doi.org/xx.yyyy/zz>, to be published.
9. Standard for Small Punch Creep Test, Estimation of Residual Life for High Temperature Component, The Committee on High Temperature Strength of Materials JSMS, The Society of Materials Science, ISBN: 978-4-901381-38-3, Japan, 2012.
10. Altstadt, E.; Ge, H.E.; Kuksenko, V.; Serrano, M.; Houska, M.; Lasan, M.; Bruchhausen, M.; Lapetite, J.-M.; Dai, Y. Critical evaluation of the small punch test as a screening procedure for mechanical properties. *Journal of Nuclear Materials*, vol. 472, pp. 186-195, 2016, <https://doi.org/10.1016/j.jnucmat.2015.07.029>.
11. Holmström, S., et. al, Determination of high temperature material properties of 15-15Ti steel by small specimen techniques, EUR 28746 EN, <https://dx.doi.org/10.2760/259065>.
12. Holmström, S., et. al., Test methodologies for determining high temperature material properties of thin walled tubes, EUR 28642 EN, <https://dx.doi.org/10.2760/702821>.
13. Holmström, S.; Simonovski, I.; Ripplinger, S.; Altstadt, E.; Delville, R.; Serrano, M.; Radu, V., Tensile and creep property determination of 15-15Ti fuel cladding steel by small punch testing, International Conference on Life Management and Maintenance for Power Plants, VTT TECHNOLOGY 261, 2016.
14. Delville, R.; Stergar, E.; and Verwerft, M., Results of a new production of nuclear-grade 1.4970 15-15Ti stainless steel fuel cladding tubes for GEN IV reactors in 22nd International Conference on Nuclear Engineering ICONE22. Prague, Czech Republic July 7-11, 2014. ASME.
15. [Catalog] Altstadt, E.; Houska, M (2018): Uniaxial tensile tests at room temperature on 24%CW 1515Ti, version 1.0, European Commission JRC, <http://dx.doi.org/10.5290/28>.
16. [Catalog] Altstadt, E.; Houska, M (2018): Uniaxial tensile tests at room temperature on 46%CW 1515Ti, version 1.0, European Commission JRC, <http://dx.doi.org/10.5290/29>.
17. [Catalog] Holmström, S. (2016): Uniaxial tensile data for P91 in the temperature range 20°C to 600°C, version 1.0, European Commission JRC Institute for Energy and Transport, <http://dx.doi.org/10.5290/6>.
18. ASTM work item WK61832, "New Test Method for Small Punch Testing of Metallic Materials", <https://www.astm.org/DATABASE.CART/WORKITEMS/WK61832.htm>.

19. Bruchhausen, M.; Holmström, S.; Simonovski, I.; Austin, T.; Lapetite, J.-M.; Ripplinger, S. and F.de Haan, Recent developments in small punch testing: Tensile properties and DBTT. *Theoretical and Applied Fracture Mechanics*, vol. 86, Part A, pp. 2-10, 2016, <https://doi.org/10.1016/j.tafmec.2016.09.012>.
20. Holmstrom, S, et Al. Small punch creep testing for material characterization and life time prediction, 10th Liege Conference: Proc. Materials for Advanced Power Engineering 2014, ISSN 1866-1793, pp. 627-635 (2014).
21. Simonovski, I.; Holmström, S.; Bruchhausen, M. Small punch tensile testing of curved specimens: Finite element analysis and experiment. *International Journal of Mechanical Sciences*, vol. 120, pp. 204-213, 2017, <https://doi.org/10.1016/j.ijmecsci.2016.11.029>.
22. ABAQUS 6.14-2, Dassault Systemes, 2015.
23. Simonovski, I. et Al., Determining the Ultimate Tensile Strength of Fuel Cladding Tubes by Small Punch Testing, JNM_2018_131, To be published.
24. [Catalog] Holmström, S (2018): Small Punch tests on 24%CW 1515Ti (curved samples) RT-800°C, version 1.0, European Commission JRC, <http://dx.doi.org/10.5290/27>.
25. [Catalog] Holmström, S (2018): Small Punch tests on 46%CW 1515Ti (curved samples) RT-800°C, version 1.0, European Commission JRC, <http://dx.doi.org/xx.yyy/zz> to be published.
26. Campitelli, E.N., et Al, Assessment of the constitutive properties from small ball punch test: experiment and modeling, *Journal of Nuclear Materials* 335 pp. 366–378, 2004.